

# MODEL SHAKING TESTS AND NUMERICAL SIMULATION ON NONLINEAR RESPONSE OF RIGID EMBEDDED FOUNDATIONS

Jun'ichi TOHMA\*, Keizo OHTOMO\* and Takahiro IWATATE\*\*

The purpose of this study is to confirm the applicability of the dynamic nonlinear soil-structure interaction (SSI) analysis for a rigid foundation embedded in soil deposit under strong earthquake ground motions. Shaking table tests were carried out, utilizing ground model made of clean sand and foundation model made of steel. Using the shear strain dependency of the shear modulus and damping determined from the soil tests, axisymmetric FEM analysis were performed taking account for the primary and secondary nonlinear response. From the comparison of the shaking test results and the numerical simulations, it was confirmed that the SSI analysis showed fairly good agreement with test results up to the soil strain level of  $10^{-3}$  order.

*Keywords*: seismic design, soil-structure interaction, embedded foundation, nonlinear response, model test, finite element method

## 1. INTRODUCTION

This paper describes one part of a research program for demonstrating methods for assessing aseismicity of nuclear power plant buildings and their foundations to be sited on the Quaternary deposit<sup>1)</sup>. The part of the program to be described here relates to the dynamic responses of embedded foundations on a soft ground. In particular, this paper discusses experimental investigation of the nonlinear responses of the foundations when subjected to strong earthquakes.

The authors previously conducted forced vibration tests on a concrete block placed on an actual ground with a vibrator by varying the depth of embedment of the block. We also conducted seismic observation of the block. With these tests and observation, we examined the embedment effect<sup>2)</sup>. As a result, we found that when the depth of embedment was made deeper, the amplitude of the block vibration decreased and the natural frequency of the coupled system increased. Moreover, we demonstrated that forced vibration tests can be simulated by an axisymmetric finite element analysis. In this series of forced vibration tests and seismic observations, however, the vibration amplitudes were extremely small when compared with those of the design earthquake motion for the nuclear power plant buildings. The strains induced in the soil were estimated to be as small as  $10^{-5}$  or under.

Soft ground is expected to show nonlinear

response when subjected to strong seismic motions corresponding to the design earthquake motion. According to some case studies, the dynamic shearing strain of the ground near the foundation is calculated to reach as high as  $10^{-3}$  when subjected to an input seismic motion of 300 to 400 Gal at the free rock surface. It, therefore, is necessary to assess the embedment effect of the foundation by properly considering the nonlinear response characteristics of the ground in such a range of large strains.

To experimentally examine such nonlinear phenomena, model vibration tests with a shaking table are effective. In the past many model vibration tests were made to examine the embedment effect of rigid foundations. In most of such experiments, however, elastic materials such as silicon rubber were used as the soil material<sup>3)-5)</sup>. With such experiments, it was confirmed that the embedment reduces the amplitude of the foundation vibration and shifts the natural frequency of the coupled system towards the shorter period side. Few studies, however, refer to the nonlinearity of the soil. Yano, et al<sup>6)</sup>. conducted model vibration tests by paying attention to the nonlinearity of backfill, and discussed the effects of the sliding and separation of the embedded portion on the responses of the structure. In their study, sand was used as the backfill, and the nonlinearity of the material was considered. Silicon rubber, however, was used for the bearing stratum model to facilitate the interpretation of the experiment. As a result, the nonlinear response of the soil as a whole was not touched upon. Matsuda and Goto<sup>7)</sup> used a large-sized shearing soil container to conduct forced vibration experiments concerning the dynamic interaction between a sand ground and a

\* Member of JSCE, M. Eng., Central Research Institute of Electric Power Industry(1646, Abiko, Abiko-shi, Chiba 270-11)

\*\* Member of JSCE, Dr. Eng., Central Research Institute of Electric Power Industry

concrete block. The sand ground in the soil container showed clear nonlinearity, but no mention was made of the embedment effect of the block.

In view of the present state as discussed above, we decided to make a sand ground in a shearing soil container to conduct model vibration tests on an embedded rigid foundation. The dynamic response of the foundation would be examined in a wide range of vibration level corresponding to small strain to large strain of the sand ground. It was intended to extend and apply the axisymmetric finite element analysis, of which applicability to the small strain range had been confirmed, to nonlinear problems. Thus the model vibration tests under strong seismic force would be numerically simulated to examine the effects of the ground nonlinearity on the embedment.

## 2. EXPERIMENTAL METHOD

A sand ground was formed in a cylindrical shearing soil container of 300 cm in diameter and 150 cm in height. A rigid foundation in the form of a 30-cm cube was placed on the ground, and model vibration tests were made by varying the depth of embedment of the foundation.

The large-sized shearing soil container used in the experiment is shown in Fig.1. This container is designed to reproduce, on the shaking table, the shear deformation which a horizontal ground will experience when it receives shear waves (SH waves) in the vertically upward direction. To be more specific, the circumference of the soil container consists of a rubber wall of 7 mm in thickness reinforced with canvas. The soil container, therefore, is capable of following the horizontal displacement of the ground in the container, at every depth. The rubber wall is reinforced with steel rings to suppress its lateral swell due to the soil pressure.

The model foundation is a solid steel one. Its mass is 212 kg, and its center of gravity is at the center of its geometrical shape. Steel rather than concrete was selected for the material of the foundation to increase its mass. This, in turn, would reduce the natural period of the coupled system of the foundation and the ground so that it would come into the possible frequency range of the shaking table.

Mountain sand, being decomposed weathered granite, from Gifu Prefecture (hereinafter called Gifu sand) was used to build a ground with water content of 8~10% in the soil container. The basic physical properties of Gifu sand include: sand content 99% ; silt and clay content 1 % ; maximum grain size 0.84 mm; uniformity coefficient 1.59 ;

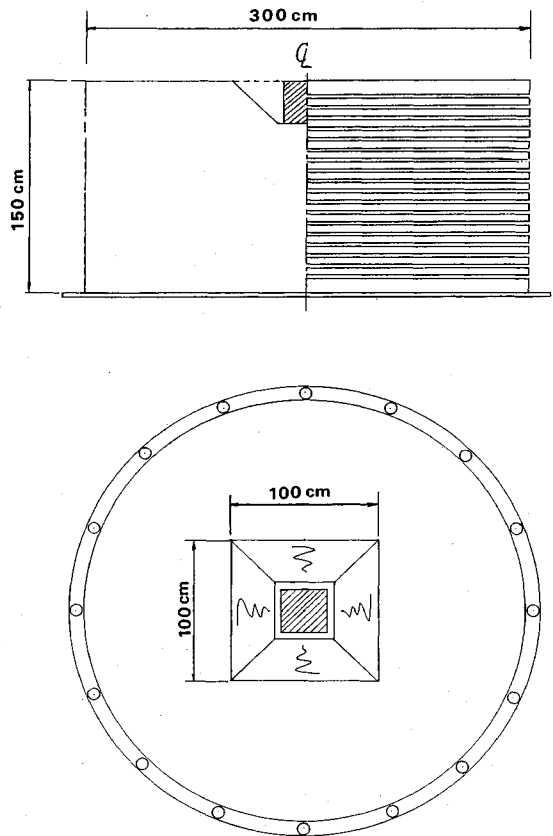
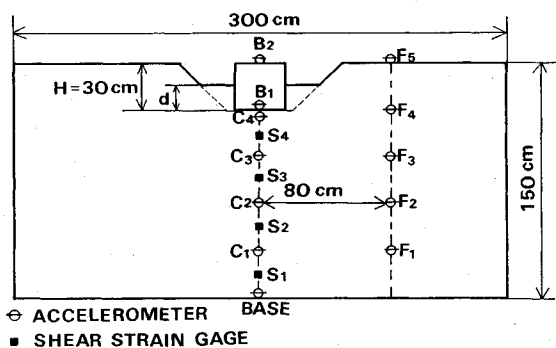


Fig.1 A cylindrical large soil container on the shaking table

maximum void ratio 1.126 ; and minimum void ratio 0.717.

Laboratory tests have been made on its dynamic deformation characteristics<sup>9)</sup>. The physical properties of the in-situ ground and those of the ground in the soil container do not necessarily agree well with each other. Even if all of their properties virtually agreed with each other, the in-situ ground and the ground in the container would differ greatly in the deformation characteristics because of the large difference in the confining pressure. Since the shear modulus and reference strain of sand are proportional to the square root of the confining pressure, Kokusho and Iwatate<sup>9)</sup> proposed a rule of similitude which is applicable to model vibration tests. According to this rule, when the shaking frequency is multiplied by  $\lambda^{0.75}$  ( $1/\lambda$  : geometrical reduced scale), the nonlinear response of a ground of which thickness is  $\lambda$  times of that of the model sand layer can be reproduced. In this case, as the similitude ratio for acceleration is 1, the similitude ratio for strain is  $1/\lambda^{0.5}$ . In our study, because of some constraints including the capacity of the shaking table, the experiment was done with



**Fig.2** The vertical cross section of the model ground-foundation system

$\lambda^{0.75}=5$ . In other words, the time axis of the seismic wave was reduced to one fifth.

The model ground was compacted with a vibrator for every 30 cm of the layer thickness. Sand samples were taken at 3 points from each layer by means of a thin wall sampler to measure the density. The mean density of the sand was  $1.378 \text{ t/m}^3$ . The mass of the entire ground was 14.6 t and was adequately large relative to that of the model foundation.

A recess of 30 cm deep was formed at the center of the top surface of the ground, and the model foundation was placed in the recess. The same ground material was used for backfilling around the foundation. The backfill up to the specified elevation was sufficiently compacted by a vibrator. The reason for selecting such an installation method was to keep the elevation from the bottom of the soil container up to the bottom of the model foundation (or thickness of the ground directly beneath the foundation) constant. We expected that it would clarify the embedment effect of the soil around the sides of the foundation. In contrast to it, the depth of placement of the foundation might be varied to examine the embedment effect. In that case, however, the input seismic motion to the bottom of the foundation would vary significantly, making it difficult to examine the embedment effect of the soil around the sides of the foundation. It should be noted that the reduction in input seismic motion depends on the installation level of the foundation, and is one of the embedment effects. That effect is very important, but in our experiment, the depth of the placement of the foundation was kept unchanged to clarify the primary target of our investigation.

The standard arrangement of measuring points for the foundation placed in the soil container is shown in Fig.2.

The height of the backfill, namely, the embedment depth of the foundation, was varied within a

range from 0 to 30 cm to conduct the experiments as will be explained below. This paper mainly discusses the major results of (3) and (4).

### (1) Free Oscillation Test by Hammering

To clarify the dynamic characteristics (natural frequency and logarithmic decrement) of the foundation when subjected to minute strains of the ground, a slight horizontal impact was given to the foundation in the horizontal direction by a rubber hammer. Then the free oscillation of the foundation was measured.

### (2) Excitation of the Foundation Top with a Vibrator

A small-sized motor-operated vibrator was mounted on the top of the foundation. Then the foundation was subjected to an excitation test wherein the frequency was varied while the eccentric moment was kept constant. The exciting force was greater than that of the hammering and was able to resonate the ground. The test was designed to obtain the resonance curve of the foundation-soil system.

### (3) Sinusoidal Excitation with a Shaking Table

While the accelerating amplitude of the shaking table was kept constant, the frequency was increased stepwise to examine the steady-state response of the foundation-soil system. The test was intended to obtain the resonance curve and phase difference at each measuring point, and in turn to clarify the frequency response characteristics and natural vibration mode of the system.

### (4) Seismic Wave Excitation with the Shaking Table

To examine the response of the foundation-soil system to seismic wave input, the system was subjected to excitation on the shaking table. The input seismic wave for the shaking table was El Centro Wave (1940, NS) of which time axis was reduced to one fifth and the duration was 5 seconds. The maximum acceleration was set stepwise from 20 Gal up to 640 Gal to obtain responses for a wide range of ground strains. Excitations with 80 Gal, 160 Gal and 320 Gal are mainly discussed in this paper. The results of the seismic wave excitation will be used as verification data for numerical simulation.

## 3. RESULTS OF SINUSOIDAL EXCITATION WITH THE SHAKING TABLE

### (1) Frequency Response of the Ground

The horizontal ground was subjected to sinusoidal excitation before a recess was made in the ground. Fig.3 shows resonance curves. The response ratio of the ground surface acceleration (F5) to the excitation acceleration (BASE) is taken

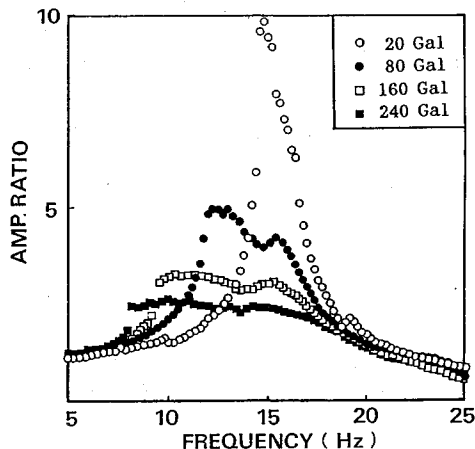


Fig.3 The resonance curves of the ground obtained from steady state response

against the frequency. The results of four cases are shown together, of which half amplitudes of the exciting acceleration were 20 Gal, 80 Gal, 160 Gal and 240 Gal, respectively. It is clear, from this figure, that when the exciting force is increased, the resonant frequency of the ground will shift to the lower frequency side, and the response ratio will decrease. In other words, the nonlinearity of the sand will appear. In Fig.3, the second peak at the frequency of 15-16 Hz is an amplification that should not occur if the shearing vibration were an idealistic one. An investigation revealed that the frames (rings) of the shearing soil container vibrate ovally in a plane in that mode.

We attempted, in the following manner, to identify the average nonlinear characteristics of the ground as a whole from the data of resonance.

First, the average shear modulus  $G$  can be obtained from Eq. (1) by using the respective resonant frequencies.

$$G = \rho V_s^2 = \rho (4Hf_0)^2 \dots \dots \dots (1)$$

- where  $\rho$  : sand density ;
- $V_s$  : average shear wave velocity of sand ;
- $H$  : thickness of sand layer ; and
- $f_0$  : resonant frequency of sand layer.

On the other hand, the average shearing strain  $\gamma$  of the ground as a whole can be obtained from Eq. (2) by using the resonant displacement amplitude. Hence  $G$  and  $\gamma$  can be related with each other.

$$\gamma = \frac{u}{H} \dots \dots \dots (2)$$

Where  $u$  : half amplitude of the relative displacement of the ground surface at the primary resonance of the ground. The value of  $u$  is calculated from the next equation by using the record of the accelerometer (F5).

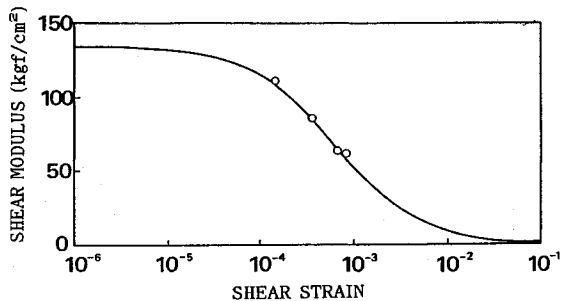


Fig.4 The strain dependency of the shear modulus of the ground determined from the shaking table tests

$$u = \frac{\ddot{u}}{(2\pi f_0)^2} \dots \dots \dots (3)$$

Where  $\ddot{u}$  : half amplitude of the absolute acceleration of the ground surface at the primary resonance of the ground. The response of the ground surface at resonance has a phase difference of 90 degrees relative to the movement of the shaking table. Thus Eq. (3) shows the relative displacement.

Eq. (2) assumes that the distribution of ground displacement in the direction of depth is a linear distribution in the form of a reversed triangle. This assumption seemed to be mostly adequate on the basis of the record of acceleration in the ground in the direction of depth at the primary resonance.

Fig. 4 shows the relationship between the shear modulus and the shear strain obtained in the above-mentioned manner. This relationship was approximated by Eq. (4) of Hardin-Drnevich type. The parameters  $G_0$  and  $\gamma_r$  were determined by the least squares method. The results are indicated on the diagram.

$$G = G_0 \frac{1}{1 + \gamma/\gamma_r} \dots \dots \dots (4)$$

- where  $G_0$  : initial shear modulus (=133.5 kgf/cm<sup>2</sup>) ; and
- $\gamma_r$  : reference strain (=6.6 × 10<sup>-4</sup>).

In this paper, we assumed, for convenience, that Eq. (4) holds, and extrapolated the value of  $G_0$ . The proper method, however, is to determine it from the results of the elastic wave exploration and density logging, or from the results of the soil tests (such as triaxial compression test or resonant-column test) in a very small strain range. The  $G_0$  values obtained by these methods should agree with each other. In practice, however, they differ from each other in many cases. The discussion of this problem is out of the scope of this paper and is omitted.

**(2) Frequency Response of the Foundation**

Fig.5 is an example of resonance curve wherein the acceleration response ratio of the horizontal

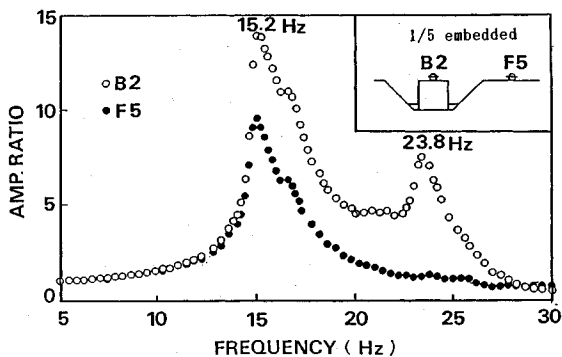


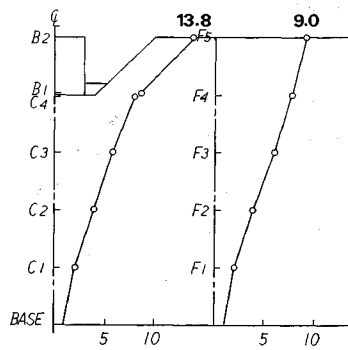
Fig. 5 The resonance curves of the soil-foundation system subjected to 20Gal input motion

movement of the foundation top (B2) to the input (BASE) is plotted against frequency. It is the case of a shallow embedment of 6 cm (one fifth of the total height of the foundation). The input acceleration amplitude is constant at 20 Gal. The diagram also shows the ground surface horizontal motion response (F5) which was measured at the same time. The amplification of both the foundation and the ground was significant at the frequency of 15.2 Hz. There was an amplification of the foundation at 23.8 Hz.

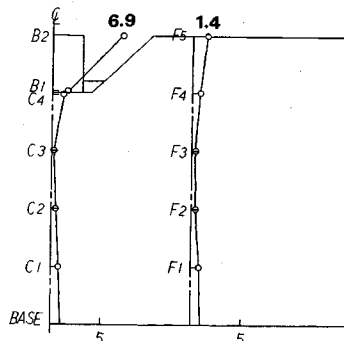
Fig. 6 (a) shows the distribution of maximum acceleration response ratio at 15.2 Hz. This is judged to be the resonance of the ground itself. Fig. 6 (b) is the distribution of maximum acceleration response ratio at 23.8 Hz. This is judged to be the resonance of the coupled system. As for the vibration of the foundation, when the ground was resonant, the vibration of the foundation was excited by the primary shear mode of the ground. When the coupled system was resonant, the vibration mode of the foundation was different from that of the ground. The mode of the coupled system may be considered as the sway and rocking vibrations of the foundation. Under the conditions of the present experiment, the maximum response of the foundation occurred not at the natural frequency of the coupled system (23.8 Hz) but at the primary resonance frequency of the ground (15.2 Hz).

#### 4. DYNAMIC DEFORMATION CHARACTERISTICS OF SAND UNDER LOW CONFINING PRESSURE

Nonlinear physical properties of Gifu Sand used in the model vibration tests were determined for the seismic response analysis that will be described later. The physical properties for the analysis were mainly determined on the basis of the results of hollow cylinder torsion tests corresponding to the



(a) at frequency 15.2 Hz



(b) at frequency 23.8 Hz

Fig. 6 The normalized amplification distribution of the soil-foundation system subjected to 20Gal input motion(1/5 embedded)

low confining pressure of the model vibration tests. The results of the investigation of 3. (1) were also considered.

In the hollow cylinder torsion tests, test specimens were hollow cylinders having the outer diameter of 100 mm, inner diameter of 60 mm, and height of 100 mm. The isotropic consolidation stress  $\sigma'_c$  prior to the loading of the dynamic stress was set in five stages with the range from 0.05 to 0.30 kgf/cm<sup>2</sup>. The water content  $w$  of the specimen was 8%. The initial void ratio  $e_0$  was set in five stages within the range from 0.7 to 1.2. Dynamic stresses were applied to the specimen, without draining, under various conditions. The frequency of the dynamic stress was 0.1 Hz, and the number of cycles (N) was up to 30 cycles.

In the model vibration tests, the mean void ratio  $e_0$  of the ground as a whole was 0.92, and the water content  $w$  was 8-10%. The confining pressure was considered to be distributed within the range from 0 to 0.14 kgf/cm<sup>2</sup> depending on the depth (the coefficient of earth pressure at rest  $K_0$  was assumed to be 0.5). These conditions meet the above-mentioned conditions of the hollow cylinder torsion tests.

The strain dependency of the shear modulus

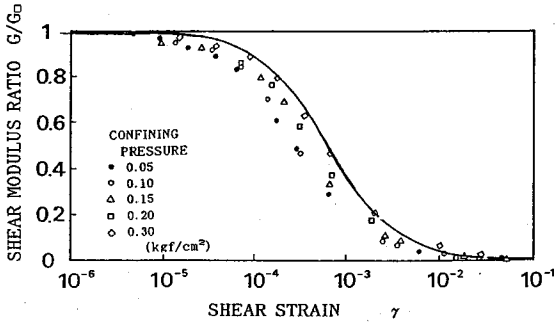


Fig.7 The strain dependency of the shear modulus ratio

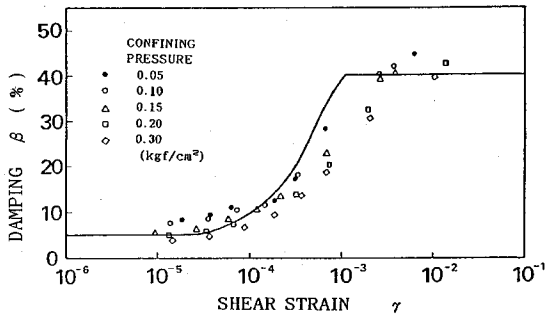


Fig.8 The strain dependency of the damping

ratio  $G/G_0$  is shown in Fig.7 for the test case of which void ratio was closest to that of the model ground. The lower was the confining pressure, the greater was the tendency of the shear modulus ratio to decrease. Eq. (4) determined by the model vibration tests is also plotted by a solid line in Fig.7. According to it, the  $G/G_0$ - $\gamma$  relationship determined by Eq. (4) represents well the decreasing tendency of the test values. The magnitude, however, seems to be close to the upper limit of the test values.

Fig.8 relates to hysteresis damping, and shows the strain dependency of the equivalent viscous damping coefficient. The lower was the confining pressure, the greater was the damping coefficient. The  $\beta$ - $\gamma$  relationship to be used in seismic response analysis is plotted by a solid line in the diagram. With regard to the curve for the analysis, the lower limit of  $\beta$  was set at 5%, and the upper limit at 40%. The relationship in the intermediate strain region was approximated by the following equation :

$$\beta = \beta_{\max} (1 - G/G_0) \dots\dots\dots (5)$$

Where  $\beta_{\max}$  : Assumed maximum damping coefficient (60%) ;  
 $G/G_0$  : Shear modulus ratio, determined from Eq.(4).

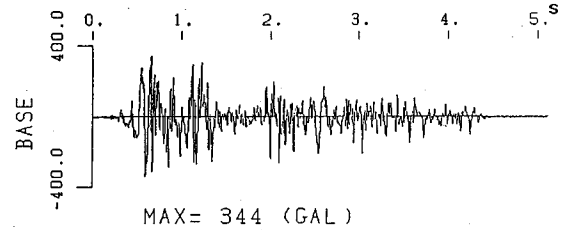


Fig.9 An acceleration time trace of the scaled input motion

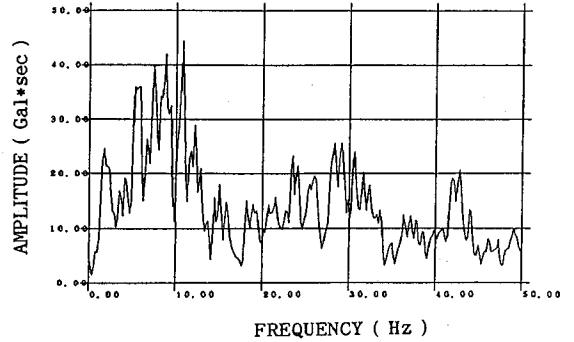


Fig.10 Fourier spectrum of the scaled input motion

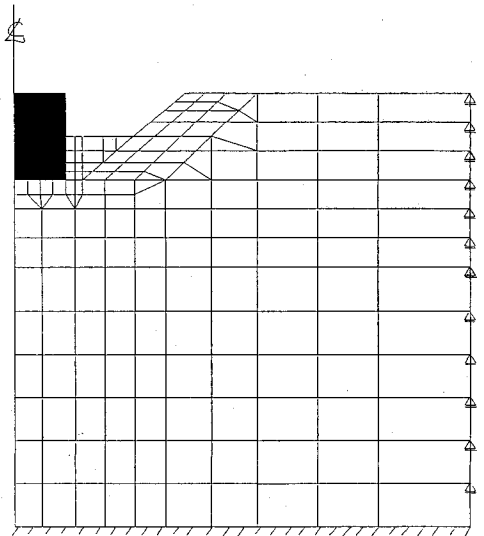


Fig.11 An axis-symmetric finite element model of the soil-foundation system

## 5. SEISMIC WAVE EXCITATION EXPERIMENT RESULTS AND NUMERICAL SIMULATION

The results of the seismic wave excitation and the results of its numerical simulation will be discussed together in this section. The numerical simulation was made by inputting the acceleration waveform of the shaking table into the bottom fixed boundary of the FEM model which will be explained later.

An example of input acceleration waveform is shown in Fig.9. Fig.10 shows the Fourier spectrum of the input waveform. The analysis was made up to 50 Hz in the frequency domain.

**(1) Modelling of the Soil-Foundation System**

A soil-structure response analysis program "CRAS" was used to examine the dynamic response of the soil-structure system. CRAS uses the complex elastic modulus indicated by the following equation as the shear modulus for the axisymmetric solid element representing the ground<sup>10)</sup>.

$$G^* = G(1 - 2\beta^2 + 2i\beta\sqrt{1 - \beta^2}) \dots \dots \dots (6)$$

where  $i = \sqrt{-1}$ .

We modelled the entire ground in the soil container as a cylinder to approximately represent the three-dimensional effect. The frames of the soil container were not modelled since they are light and have low rigidity. The actual shape of the foundation is a cube, but it was replaced with an equivalent cylinder having the same base area. The division into elements is shown in Fig.11. With regard to the contact between the ground and the foundation, we assumed that the deformation is continuous at each node. Any sliding and/or separation across the contact surface, therefore, are not considered in the analysis. In view of the structural characteristics of the soil container, the ground bottom boundary was fixed, and the lateral boundary of the ground were approximated with horizontal rollers.

**(2) Initial Stress Analysis**

Prior to the seismic response analysis, it was decided to consider the confining-pressure dependency of the initial shear modulus  $G_0$ . The changes in  $G_0$  depending on the dead load of the sand was calculated in the following manner and assigned to each element.

As shown in Fig.4, our basic approach was to use a value of  $G$ - $\gamma$  curve extrapolated to a very small strain ( $\gamma = 10^{-6}$ ). We adopted a constant value of  $G_0 = 133.5 \text{ kgf/cm}^2$  in the direction of depth. Next, we assumed that  $G_0$  is proportional to the square root of the confining pressure. Then we redefined the distribution of  $G_0$  in the direction of depth, with a condition that the natural frequency of the ground determined from the mean  $G_0$  not be altered. As a result,  $G_0$  can be represented by the following equation

$$G_0 = 495\sigma^{0.5} (\text{kgf/cm}^2) \dots \dots \dots (7)$$

where  $\sigma$  : mean principal stress (kgf/cm<sup>2</sup>).

Moreover, the increase in the confining pressure due to the weight of the foundation (contact pressure :  $0.236 \text{ kgf/cm}^2$ ) was taken into considera-

tion; on the basis of Eq. (7), static stress analysis was made with the axisymmetric finite element analysis. The shear modulus thus obtained was denoted by  $G'_0$ . The ratio of  $G'_0$  to  $G_0$  without considering the foundation weight,  $G'_0/G_0$ , rose to about 1.7~2.3 for the ground element contacting the bottom of the foundation.

**(3) Treatment of Nonlinearity of Sand**

We used the relationships plotted by solid lines in Fig.7 and Fig.8 as the curves indicating the strain dependencies of the shear modulus  $G$  and damping coefficient  $\beta$  of the sand for all ground elements. Thus the nonlinearity was examined by the equivalent linear analysis based on the repeated convergence calculation for each ground element. The process is identical to, for example, FLUSH<sup>11)</sup>. In the case of CRAS being an axisymmetric analysis, however, each element has a strain of 6 components. The two-dimensional maximum shearing strain  $\gamma_{\text{max}}$  in the plane perpendicular to the accelerating direction was calculated by the following equation.

$$\gamma_{\text{max}} = \sqrt{(\epsilon_r - \epsilon_z)^2 + \gamma_{rz}^2} \dots \dots \dots (8)$$

The value of  $\gamma_{\text{max}}$  was multiplied by the coefficient of effective strain amplitude to obtain the effective strain  $\gamma_{\text{eff}}$ . The coefficient of effective strain amplitude is a coefficient for approximately corresponding an irregular response (such as seismic response) to an equivalent steady-state response (such as cyclic triaxial test). The ordinary value used in practical engineering is about 0.65, but the optimal value depends on the vibration waveform and the characteristics of the ground. When the coefficient of effective strain amplitude is changed, the results of the response analysis may be changed<sup>12)</sup>. At present, however, it is not possible to set the optimal value prior to the analysis. We, therefore, used a conventional value of 0.65.

**(4) Comparison of Analytical Results and Experimental Results Concerning Maximum Acceleration Distribution**

Fig.12 shows the maximum acceleration distributions of the foundation when the El Centro wave of 80 Gal was inputted to verify the precision of the simulation for various embedment depths. In the diagram, (a) represents the embedment of 6 cm, (b) half embedment, and (c) total embedment. The tendency of the maximum acceleration response of the foundation to decrease a little with the embedment, which was observed in the experiment, was represented by the simulation. This tendency to decrease, however, was not as conspicuous as was the case of the excitation test of the foundation top. When the excitation is given

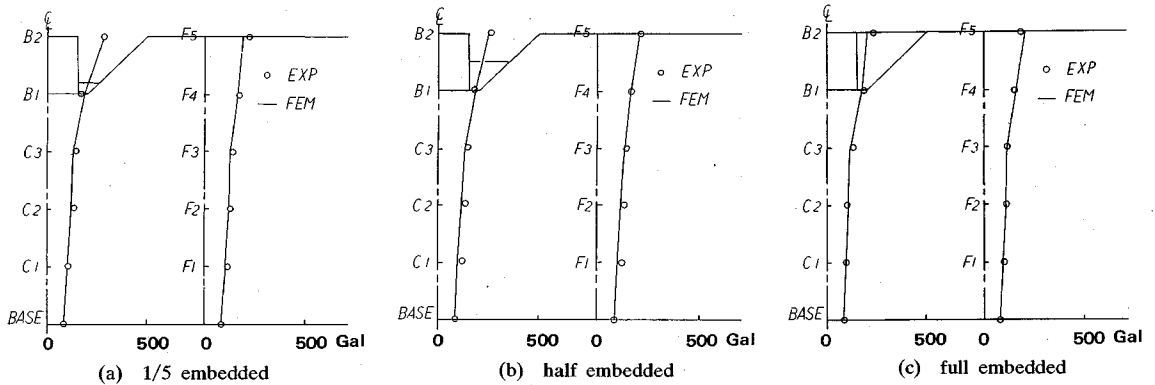
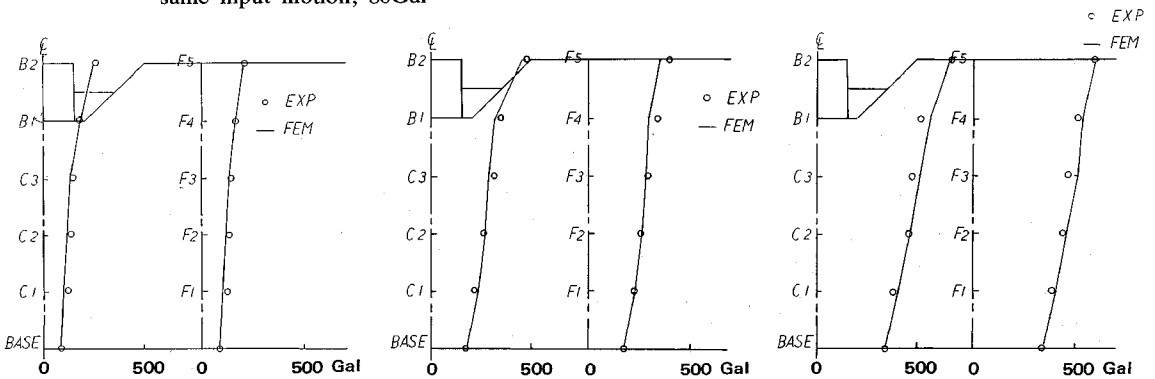


**Fig.12** The maximum acceleration distribution from the experimental and simulated results under the same input motion; 80Gal



(a) The maximum input motion : 80 Gal (b) The maximum input motion : 160 Gal (c) The maximum input motion : 320 Gal

**Fig.13** The maximum acceleration distribution of from the experimental and simulated results under the same embedment depth ; half embedded

to the ground in the upward direction as was the case of our experiment, the foundation responds to the vibratory response of the entire ground. As a result, the difference in the foundation response due to a change in the embedment depth seems to be concealed by the response of the ground itself.

Fig.13 shows the maximum acceleration response distributions of the ground and the foundation when the foundation was half embedded. The diagram is to verify the accuracy of the simulation for varied magnitudes of the input acceleration. In the diagram, (a) represents the El Centro wave input of 80 Gal, (b) the same input of 160 Gal, and (c) the same input of 320 Gal. The analytical values agree well with the experimental values at the varied input levels.

### 6. DISCUSSION ON NONLINEAR RESPONSE OF THE SOIL-STRUCTURE SYSTEM

Fig.14 shows the amplification ratio ( $B2/BASE$ ) which is the maximum horizontal acceleration of the foundation top divided by the maximum acceleration of the shaking table. The greater was

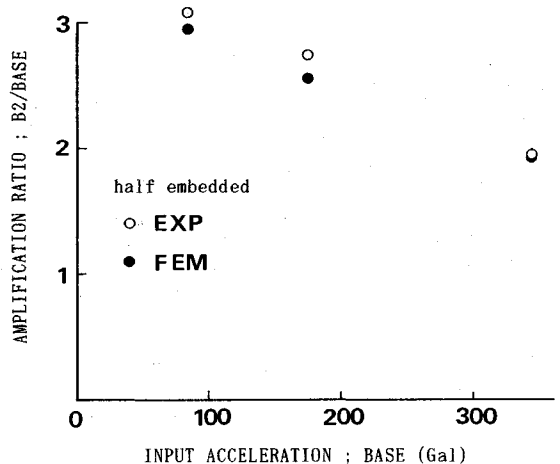
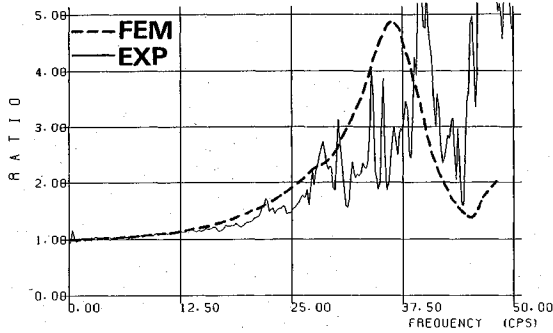


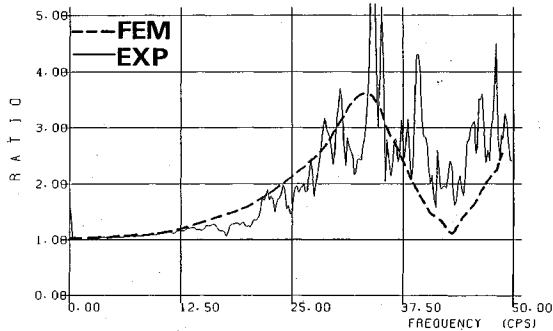
**Fig.14** The maximum amplification ratio ( $B2/BASE$ ) versus the maximum BASE acceleration

the shaking acceleration, the greater was the tendency of the amplification ratio to decrease. The main cause of this phenomenon must be the increase in the hysteresis damping of the sand. Concerning this tendency, the analytical values,

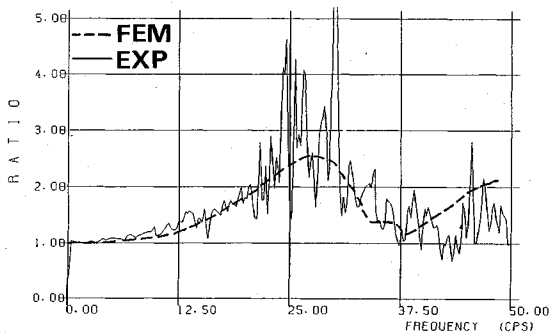




(a) The maximum input motion : 80 Gal



(b) The maximum input motion : 160 Gal



(c) The maximum input motion : 320 Gal

**Fig.15** The transfer functions (B2/F4) obtained from the experiment and the simulation

although being based on the equivalent linear method, show a relatively good correspondence with the experimental values. Hence it may be judged that the equivalent linear analysis such as one used this time gives reliable analytical results for seismic input at least up to 300 Gal, provided that the assessment of the dynamic deformation characteristics of the ground is appropriate. The above-mentioned input corresponds, as will be explained later, to the response wherein the dynamic shearing strain of the ground is at  $10^{-3}$  level.

**Fig.15** (a), (b) and (c) relate to the case of half embedment (depth  $d = 15$  cm) and show the frequency transfer functions for the shaking

**Table 1** Grouping of the induce strain

group	strain range	$G/G_0$
I	0 to $1 \times 10^{-4}$	$> 0.9$
II	$1 \times 10^{-4}$ to $5 \times 10^{-4}$	0.9 to 2/3
III	$5 \times 10^{-4}$ to $1 \times 10^{-3}$	2/3 to 1/2
IV	$1 \times 10^{-3}$ to $5 \times 10^{-3}$	1/2 to 1/6

maximum acceleration of 80 Gal, 160 Gal and 320 Gal, respectively. The Fourier spectrum ratio (B2/F4) of the foundation top acceleration (B2) to the acceleration in the ground (F4) was selected as the frequency transfer function. The measuring point F4 was selected for the acceleration in the ground because the point is at the same depth with the bottom of the foundation. The vibration at F4 is thus considered to be the major seismic input to the foundation. In the diagrams, the solid lines indicate the experimental results, and the broken lines indicate the simulation results. The experimental results show small irregularities since the time-series record was converted into the frequency domain before calculating the spectrum ratio. In contrast, in the simulation, because of the nature of the analytical technique, the transfer function is smooth in the frequency domain. Although such differences exist between the experimental results and the analytical results, both results clearly showed the shift of the peak of the transfer function towards the lower frequency side and the relative decrease in the amplification ratio with the increase in the exciting acceleration.

The above-mentioned peak of the transfer function can be interpreted as the natural frequency (sway and rocking vibrations) of the coupled system. Hence the dependency of this natural frequency on the exciting acceleration may be interpreted as the indication of the effects of the ground nonlinearity on the dynamic interaction.

**Fig.16** shows the distribution of the ground's maximum strain  $\gamma_{max}$  obtained by analysis. The magnitude of the strain is classified into four kinds, i.e. Group I ~ IV, and the kind of each ground element is identified. The magnitude of such strains can be related to the decrease ratio of shearing modulus ( $G/G_0$ ) by converting the strain magnitude into the effective strain  $\gamma_{eff}$  and following Eq.(4). The results are shown in Table 1.

Concerning **Fig.16** (a), (b) and (c), it is a matter of course that the strain level of the entire ground increased with the increase in the exciting acceleration. One noticeable feature is that strains are concentrated (namely, slackness) to the ground elements that contact the side faces and the bottom corners of the foundation. It is also clear that,

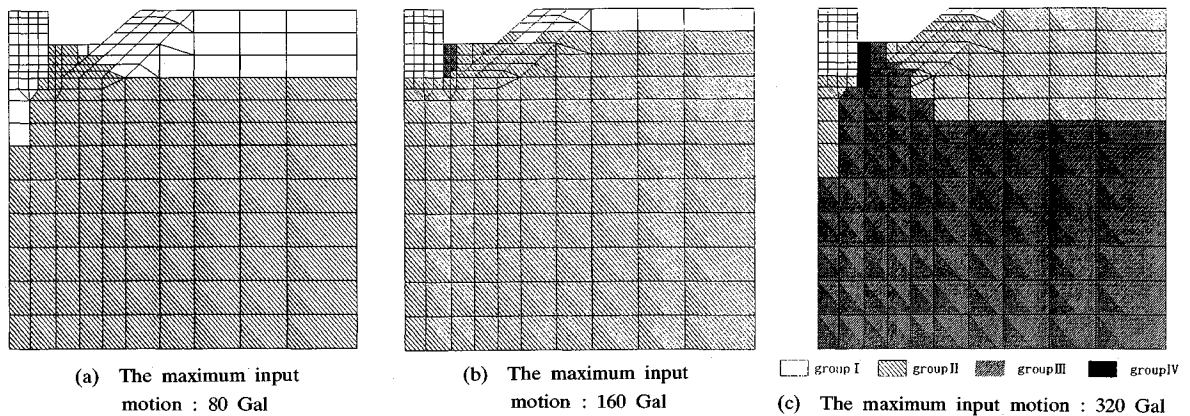


Fig.16 The maximum shear strain distribution induced in the soil; Half embedment( $d=15\text{cm}$ )

directly beneath the foundation, the slackness is hard to occur since the rigidity of the ground is increased by the contact pressure.

According to the results of a separate investigation by the authors<sup>1)</sup>, when a sand and gravel ground with shear wave velocity  $V_s$  of 300 to 500 m/s is subjected to seismic input of 300 to 400 Gal at free rock surface, the strain generated in the ground is analytically expected to be  $10^{-3}$  level. Of the present model vibration tests, the case with the exciting acceleration of 320 Gal (Fig.16 (c)) is close to the above-mentioned analytical result from the viewpoint of the shearing strain magnitude. In this case, the strain of Group III was generated in about two thirds of the ground thickness in a zone which is considered to be a free ground. The primary nonlinear response is dominant in this zone. Near the foundation, the strain of Group IV was generated on the side faces of the foundation. the horizontal width of this large strain zone is as large as about one third of the equivalent radius (22.6 cm) of the foundation. In succession to it, a strain zone of Group III expanded downwards slantwise. This concentration of strain due to the presence of the foundation indicates the zone has the effects of the secondary nonlinear response.

In the practical design calculation, one simple way for considering the secondary nonlinear effects in the elastic finite element method is to reduce the rigidity of the ground contacting the sides of the foundation to  $1/2-1/6$  of the convergent value of the response analysis (ex. SHAKE) of a free ground and make linear calculation. In this way, the slacking of the ground due to stress concentration can be introduced approximately. In this case, the rigidity drop zone may be assumed to be as follows: The horizontal width from the edge of the foundation is about one third of the equivalent radius of the foundation, and the depth is from the

ground surface to the bottom of the foundation. We will examine the applicability of this simplified method through the in-situ strong earthquake observation of structures in future<sup>14)</sup>.

## 7. CONCLUSIONS

The dynamic responses of an embedded foundation on a soft ground were experimentally examined with a special attention to the nonlinear responses under strong earthquakes. The depth of embedment of the foundation was varied to examine its dynamic responses to a wide range of vibrations corresponding to small and large strains in the ground. The experimental results were simulated by the axisymmetric finite element analysis to make the equivalent linear analysis. Moreover, the range of the effects of the secondary nonlinear responses was examined on the basis of the calculated strains in the ground.

The findings of this study are summarized as follows:

(1) The resonance of the ground and that of the soil-foundation system were induced by different frequencies. The resonant frequency of the soil-foundation system was higher than that of the ground under the conditions of our experiments. The resonance of the soil-foundation system was due to the natural vibration (sway and rocking vibrations) of the coupled system.

(2) The maximum acceleration at the top of the foundation induced by seismic wave excitation showed a tendency to decrease with the backfill around the sides of the foundation, although the depth of installation of the foundation was kept constant. This tendency, however, was not very conspicuous. The reason is that the response of the foundation was dominated by the vibration mode of the entire ground.

(3) The foundation and the ground were

excited with seismic wave input of various amplitude. The amplification ratio of the foundation per unit acceleration decreased with the increase in the exciting acceleration; the effects of the nonlinearity of the ground were conspicuous. The transfer functions of the foundation and the ground indicated the drop in the natural frequency of the coupled system and the decrease in the amplification ratio with the increase in the exciting acceleration.

(4) Numerical simulations of the model vibration tests were made. It was confirmed that changes in response characteristics due to the nonlinearity of the ground can be assessed satisfactorily, in terms of the maximum acceleration distributions and transfer functions, provided the assessment of the dynamic deformation characteristics of the ground is appropriate.

(5) Concerning the case of half embedment, the decrease ratio of rigidity of the ground was estimated from the strain distribution of the ground. A zone of which rigidity was not more than one half of the initial rigidity was observed in the backfill under the seismic wave excitation of up to 320 Gal. On the basis of this finding, a simple assessment method was developed. It approximates the slackness due to the stiffness degradation of the soil around the foundation.

#### REFERENCES

- 1) Iwatate, T. et al. : Study on siting technology for nuclear plant on Quaternary ground (Part 2), Report of Central Research Institute of Electric Power Industry, U20, 1991.2 (in Japanese).
- 2) Tohma, J. et al. : Forced vibration tests and earthquake observation on the dynamic response of rigid foundations, Proc. of JSCE No.446/I-19, pp.57~67, 1992.4.
- 3) Kiya, Y. et al. : Model tests on embedment effect on reactor building-Laboratory test, Proc. of Annual Conference of AIJ, (Part 1~4) pp.1079~1086, 1989.10, and (Part 5~7) pp.1379~1384, 1990.10 (in Japanese).
- 4) Yoshimura, N. et al. : Experimental study on dynamic interaction of soil and embedded structure (Part 1 and 2), Proc. of Annual Conference of AIJ, pp.513~516, 1986.8 (in Japanese).
- 5) Matsushima, Y. et al. : Shaking table test of embedded structure soil interaction and its analysis with special reference to input motion (Part 1~5), Proc. of Annual Conference of AIJ, pp.517~526, 1986.8 (in Japanese).
- 6) Yano, A. et al. : Experiments and analyses on nonlinear dynamic response of embedded building at earthquake (Part 1 and 2), Proc. of Annual Conference of AIJ, pp.509~512, 1986.8 (in Japanese).
- 7) Matsuda, T. and Goto, Y. : Experiment technique on dynamic properties of model ground in shearing stack box, Proc. of the 7th JEES, pp.792~798, 1986 (in Japanese).
- 8) Ishida, T. et al. : Static and dynamic mechanical properties of sandy materials for model test of slope failure under the condition of low confined stress, Report of Central Research Institute of Electric Power Industry, No.380045, 1981.5 (in Japanese).
- 9) Kokusho, T. and Iwatate, T. : Scaled model tests and numerical analyses on nonlinear dynamic response of soft grounds, Proc. of JSCE, No.285, pp.57~67, 1979.5 (in Japanese).
- 10) Iwatate, T. and Kokusho, T. : Development of computer program for evaluating the dynamic responses of soil-structure system during earthquake, Report of Central Research Institute of Electric Power Industry, No.380023, 1980.12 (in Japanese).
- 11) Lysmer, J. et al. : 'FLUSH'-A computer program for approximate 3-D analysis of soil structure interaction problems, EERC 75-30, Univ. of California, Berkeley, 1975.
- 12) JSCE : Dynamic analysis and earthquake resistant design, Vol.2 Dynamic analysis method, pp.90~92 and pp.201~202, Giho-do Publishing Co., Ltd., 1989 (in Japanese).
- 13) Schnabel, B. et al. : SHAKE A computer program for earthquake response analysis of horizontally layered sites, EERC 72-12, Univ. of California, Berkeley, 1972.
- 14) Tang, H.T. et al. : The Hualien large-scale seismic test for soil-structure interaction research; Trans. of the 11th Conf. on Structural Mechanics in Reactor Technology, k04/4, 1991.

(Received June 17, 1991)

## 埋込み剛体基礎の非線形応答に関する模型振動実験とその解析

当麻純一・大友敬三・岩楯敏広

本研究の目的は、軟質地盤に埋め込まれた剛体基礎について、その強震時の非線形応答を実験的に把握して、地震応答解析法の検証を図ることにある。振動台上のせん断土槽内に砂地盤を作成し、その上に模型基礎を設置して振動実験を行った。砂の動的変形特性を適切に評価することで、軸対称有限要素解析によって実験結果を説明できることを示した。これに基づき、動的相互作用で生じる地盤剛性低下の領域とその程度を考察した。